RNA-Binding Protein *ZFP36L1* Suppresses Hypoxia and Cell-Cycle Signaling

Xin-Yi Loh[1], Qiao-Yang Sun[1], Ling-Wen Ding[1], Anand Mayakonda[1], Nachiyappan Venkatachalam[1], Mei-Shi Yeo[1], Tiago C. Silva[2,3], Jin-Fen Xiao[1], Ngan B. Doan[4], Jonathan W. Said[4], Xue-Bin Ran[1], Si-Qin Zhou[1], Pushkar Dakle[1], Pavithra Shyamsunder[1], Angele Pei-Fern Koh[1], Ruby Yun-Ju Huang[1], Benjamin P. Berman[3,5], Soo-Yong Tan[6], Henry Yang[1], De-Chen Lin[7], and H. Phillip Koeffler[1,7,8]

ABSTRACT

ZFP36L1 is a tandem zinc-finger RNA-binding protein that recognizes conserved adenylate-uridylate–rich elements (ARE) located in 3′untranslated regions (UTR) to mediate mRNA decay. We hypothesized that ZFP36L1 is a negative regulator of a post-transcriptional hub involved in mRNA half-life regulation of cancer-related transcripts. Analysis of *in silico* data revealed that ZFP36L1 was significantly mutated, epigenetically silenced, and downregulated in a variety of cancers. Forced expression of ZFP36L1 in cancer cells markedly reduced cell proliferation *in vitro* and *in vivo*, whereas silencing of ZFP36L1 enhanced tumor cell growth. To identify direct downstream targets of ZFP36L1, systematic screening using RNA pull-down of wild-type and mutant ZFP36L1 as well as whole transcriptome sequencing of bladder cancer cells {plus minus} tet-on ZFP36L1 was performed. A network of 1,410 genes was identified as potential direct targets of ZFP36L1. These targets included a number of key oncogenic transcripts such as HIF1A, CCND1, and E2F1. ZFP36L1 specifically bound to the 3′UTRs of these targets for mRNA degradation, thus suppressing their expression. Dual luciferase reporter assays and RNA electrophoretic mobility shift assays showed that wild-type, but not zinc-finger mutant ZFP36L1, bound to HIF1A 3′UTR and mediated HIF1A mRNA degradation, leading to reduced expression of HIF1A and its downstream targets. Collectively, our findings reveal an indispensable role of ZFP36L1 as a posttranscriptional safeguard against aberrant hypoxic signaling and abnormal cell-cycle progression.

Significance: RNA-binding protein ZFP36L1 functions as a tumor suppressor by regulating the mRNA stability of a number of mRNAs involved in hypoxia and cell-cycle signaling.

Introduction

Urinary bladder cancer is one of the most frequently diagnosed cancers worldwide, with an estimate of 430,000 new cases and 160,000 deaths in 2012 (1). Patients with superficial non-muscle–invasive bladder cancers have prolonged survival yet frequently recur (15%–70%; ref. 2); on the other hand, tumors that invade into muscle layer [muscle-invasive bladder cancer (MIBC)] have a worse prognosis. For instance, the 3-year overall survival of patients with MIBC who recur after radical cystectomy or radiotherapy is only 6%–12% (3, 4). Because of the highly heterogeneous nature of bladder cancer, molecular profiling and classification are required to understand the pathogenesis of bladder cancer and to identify novel therapeutic targets.

Adenylate-uridylate (AU)–rich elements (ARE) are a group of instability determinants located in the 3′ untranslated regions (3′UTR) of labile RNA to control posttranscriptional regulation. Generally, AREs are categorized into three classes: class I - dispersed AUUUAs, class II - repeated AUUUAs, and class III - U-rich regions. In a variety of cancers, many ARE-containing transcripts have a prominent role in proliferation, metabolism, angiogenesis, and survival in adverse conditions such as hypoxia (5, 6). AU-rich RNA-binding proteins (AUBP) bind specifically to multimeric AUUUA sequences, leading to either stabilization or degradation of target RNA. Zinc finger protein 36 (ZFP36) family is one of the best-characterized AUBPs, consisting of *ZFP36, ZFP36L1*, and *ZFP36L2*. All three ZFP36 family members contain highly conserved tandem zinc-fingers that recognize AREs sequences in 3′UTRs of RNA (7–9). ZFP36L1 acts as an adaptor protein and interacts with RNA degradation complexes to participate in ARE-mediated RNA decay. ZFP36L1 recruits deadenylase such as CCR4 for deadenylation and delivers deadenylated RNA transcripts to P-bodies for decapping (by DCP1a and DCP2) prior to 5′-to-3′ exonucleolytic decay (by exonuclease XRN1; refs. 10–12). Meanwhile, ZFP36L1 also interacts with exosome component RRP4s for 3′–5′ decay (10).

ZFP36L1 is a downstream target of protein kinase B (PKB/AKT; ref. 13), ERK/RSK (14), and MAPK-activated protein kinase 2 (MK2; refs. 15, 16). Although phosphorylation of ZFP36L1 at conserved serine residues (serines 54, 92, 203) does not impair the binding of AREs, it causes CCR4–NOT–deadenylase complex to dissociate from targeted RNA (14) and induces ZFP36L1 complex formation with 14-

[1]Cancer Science Institute of Singapore, National University of Singapore, Singapore. [2]Department of Genetics, Ribeirão Preto Medical School, University of São Paulo, Ribeirão Preto, Brazil. [3]Center for Bioinformatics and Functional Genomics, Department of Biomedical Sciences, Cedars-Sinai Medical Center, Los Angeles, California. [4]Pathology and Laboratory Medicine, Ronald Reagan UCLA Medical Center, Los Angeles, California. [5]Department of Developmental Biology and Cancer Research, Institute for Medical Research Israel-Canada, Hebrew University-Hadassah Medical School, Jerusalem, Israel. [6]Department of Pathology, Yong Loo Lin School of Medicine, National University of Singapore, Singapore. [7]Department of Medicine, Cedars-Sinai Medical Center, Los Angeles, California. [8]National University Cancer Institute of Singapore, National University Hospital, Singapore.

Note: Supplementary data for this article are available at Cancer Research Online (http://cancerres.aacrjournals.org/).

Corresponding Author: Ling-Wen Ding, Cancer Science Institute of Singapore, Department of Pathology, Yong Loo Lin School of Medicine, National University of Singapore, 14 Medical Drive, Singapore 117599, Singapore. Phone: 65-8345-1790; Fax: 65-6873-9664; E-mail: lingwen.dlw@gmail.com

Cancer Res 2020;80:219–33

doi: 10.1158/0008-5472.CAN-18-2796

©2019 American Association for Cancer Research.

Downloaded from http://aacrjournals.org/cancerres/article-pdf/80/2/219/2796271/219.pdf by guest on 27 August 2022

3-3 protein (13, 15, 17). This form of phosphorylation-dependent protein stabilization protects ZFP36L1 from proteasomal degradation (17), which also presumably leads to a dominant-negative form of ZFP36L1 protein to stabilize target RNA, by preventing recruitment of deadenylase machinery for RNA degradation. Thus, mitogenic signaling and phosphorylation process dynamically control the post-transcription RNA decay process through ZFP36 family members and fine-tune the gene transcript network.

Recent studies suggested that ZFP36L1 plays an indispensable role in tumorigenesis. Simultaneous deletion of *Zfp36l1* and *Zfp36l2* in an experimental murine model leads to the upregulation of *Notch1* transcripts, resulting in the development of T-cell acute lymphoblastic leukemia (T-ALL; ref. 18). ZFP36L1 degrades cellular inhibitor of apoptosis protein-2 (*cIAP2*) RNA (19), suppresses the growth of Lewis lung carcinoma (20), inhibits *cyclin D1* in colorectal cancer (21) and facilitates *VEGFA* mRNA decay (22, 23). By comprehensively analyzing the pan-cancer exome sequencing data generated by TCGA etc., we found that *ZFP36L1* is significantly mutated and underexpressed in bladder cancer, which prompted us further to examine its role in tumorigenesis.

Materials and Methods

Cell lines and cell culture

Bladder cancer cell lines (HT1376, T24, J82, and UMUC3) and breast cancer cell lines (HS578T and BT474) were obtained from ATCC. All cell lines were authenticated via short tandem repeat (STR) profiles in 2015 and were tested for *Mycoplasma* regularly by PCR testing in 2019. All cell lines were stored in liquid nitrogen and cultured for less than 10 passages after STR authentication for the experiments.

Antibodies and reagents

Following antibodies were used for Western blot analyses, ZFP36L1 (sc-134091, Santa Cruz Biotechnology), BRF1/2 (#2119, Cell Signaling Technology), β-actin (A1978, Sigma Aldrich), rabbit anti-V5-Tag antibody (#13202, Cell Signaling Technology), HIF1A (GTX127309, Genetex), cyclin D1 (L2309, Santa Cruz Biotechnology), cyclin D3 (#2936, Cell Signaling Technology), E2F1 (#3742S, Cell Signaling Technology), cyclin E (#4129P, Cell Signaling Technology), CDK Antibody Sampler Kit (#9868, Cell Signaling Technology) with CDK2 (#2546, Cell Signaling Technology), and CDK4 (#12790, Cell Signaling Technology).

RNA pull-down experiments

E.coli recombinant protein expression vectors (*GST, GST-ZFP36L1, GST-ZFP36L1-Ala* mutant) were generated using pGEX-4T1 plasmid. These GST fusion proteins were purified using glutathione sepharose. Meanwhile, J82 cells were lysed with protein extraction buffer. Cell lysates were incubated with recombinant proteins for 2 hours at 4°C. RNAs bound by ZFP36L1 recombinant proteins were pulled down by glutathione sepharose beads, purified by TRIzol, and sequenced using high-throughput RNA-sequencing.

RNA sequencing and microarray analyses

Alterations of RNA expression in doxycycline-inducible *Tet-ZFP36L1* J82 cells (either with or without doxycycline), in siRNA knockdown of *ZFP36L1*, as well as in RNA pull-down of J82 cells (using the recombinant proteins of GST, wild-type GST-ZFP36L1, and GST-ZFP36L1-Ala mutant) were determined by high-throughput transcriptome-sequencing. cDNA array hybridization was conducted using Illumina Human HT-12 v4 Expression BeadChip. Pathway analysis was accomplished with Kyoto Encyclopedia of Genes and Genomes (KEGG) and Reactome databases. Real-time RT-PCR was performed to validate significantly altered genes using primers listed in Supplementary Table S1. The sequencing data were submitted to GEO database with following accession numbers: RNA pull down (GSE136179), *ZFP36L1* tet-on overexpression of 6 hours and 24 hours (GSE136181), and *ZFP36L1* siRNA knockdown (GSE136180).

Synthesis of the biotin-labeled RNA probes

Linearized DNA templates of *HIF1A, E2F1*, and *CCND1* flanked with a 5′ T7 promoter region were generated by PCR. Biotin-labeled (Biotin-16-CTP, ChemCyte) RNA sequences were prepared using T7 *in vitro* transcription (HiScribe T7 High Yield RNA Synthesis Kit, New England Biolabs).

RNA electrophoretic mobility shift assay

RNA electrophoretic mobility shift assays (RNA-EMSA) were performed using the LightShift Chemiluminescent RNA EMSA Kit (Thermo Fisher Scientific). Protein lysates of HEK293T, which were either expressing *ZFP36L1* or empty control plasmid, were extracted. Biotin-labeled RNA probes were incubated with the protein lysates for 30 minutes to allow binding of ZFP36L1 to the biotin-labeled RNA probes. Electrophoretic transfer of the RNA probes to nylon membranes was performed. Membranes were washed and blocked. Images of RNA probes were captured in the darkroom using CCD camera–based imager.

Murine xenograft model

The studies were approved by the NUS Institutional Animal Care and Use Committee (no. R18-0330). *In vivo* tumor growth was performed on female NSG mice. The tumors were harvested. Their sizes and weights were measured.

Statistical analyses

Analyses were performed using GraphPad Prism v6. $P < 0.05$ was considered as statistically significant. Differences between averages of variables were compared using the two-tailed unpaired t test for variables with normal distributions. Overall survival was computed using the Kaplan–Meier method. P values of overall survival were calculated using the log-rank test.

See also the Materials and Methods provided in Supplementary Data.

Results

ZFP36L1 is frequently mutated, epigenetically silenced, and underexpressed in bladder and breast carcinomas

To determine comprehensively the genetic alterations of ZFP36 family members, we interrogated exome sequencing data of approximately 70,000 primary cancer samples using cBioPortal pan-cancer database (24). Mutations were scattered across the proteins in all three family members (ZFP36, ZFP36L1, and ZFP36L2; Supplementary Fig. S1A). Pronounced truncating mutations (frameshifts, stop-gains, and indel deletions) are particularly identified in ZFP36L1 and ZFP36L2. These mutations are likely to lead to a loss-of-function for the encoded protein. This observation prompted us to examine the truncation of ZFP36L1 in detail. Remarkably, the majority of these truncating mutations of ZFP36L1 occurred in bladder and breast cancer samples; thus, these two cancer types were selected as our study models (**Fig. 1A**). Analyses of significantly mutated genes using

Downloaded from http://aacrjournals.org/cancerres/article-pdf/80/2/219/2796271/219.pdf by guest on 27 August 2022

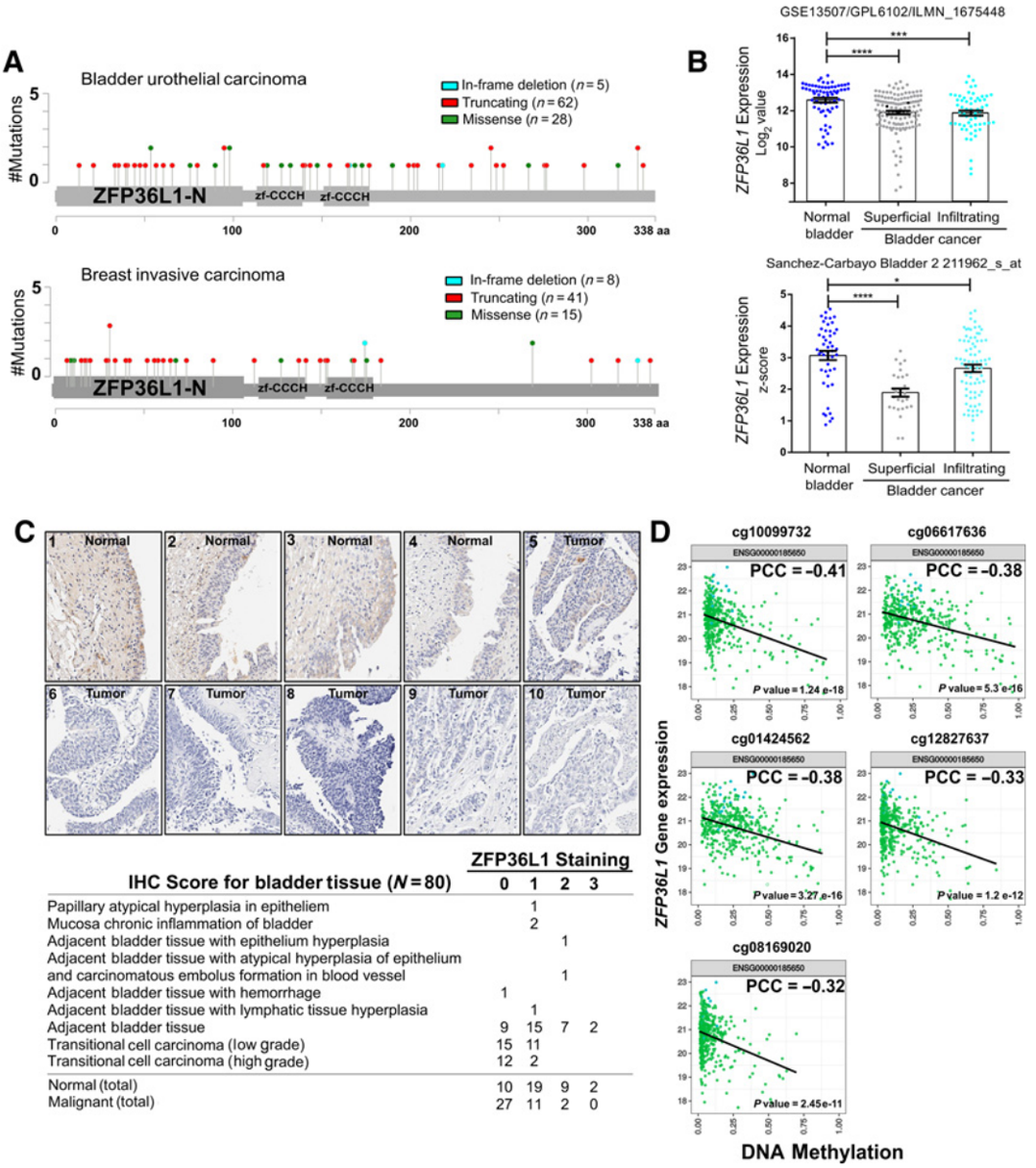

Figure 1.

ZFP36L1 is significantly mutated, epigenetically silenced, and downregulated in bladder carcinoma. **A,** Somatic mutations of ZFP36L1 in bladder and breast cancers. Diagrams show mutational patterns (in-frame deletions, missense, and truncating mutations) of ZFP36L1. The "# Mutations" on the *y*-axis denotes the number of mutations that occur at the same amino acid. The data were retrieved from cBio Cancer Genomics Portal (24). **B,** Decreased *ZFP36L1* expression in superficial and infiltrating bladder cancers compared with normal tissues. Data were obtained from Gene Expression Omnibus (GEO) and Oncomine databases. Mean ± SEM. *, $P < 0.05$; ***, $P < 0.001$; ****, $P < 0.0001$. **C,** Top, representative photos of ZFP36L1 IHC staining of bladder tumors and their adjacent normal tissues. #1, 2, and 3, adjacent normal bladder tissues; #4, urothelial hyperplasia; #5, #6, #7, and #8, low-grade papillary urothelial carcinoma; #9 and #10, infiltrating high-grade urothelial carcinoma. Magnification, ×200. Bottom, summary scoring results of the IHC staining with ZFP36L1 antibody in 40 bladder carcinoma tissues, compared with 40 normal adjacent tissues. 0, no staining; 1, weak staining; 2, moderate staining; 3, strong staining. *N*, number of bladder IHC samples. **D,** Scatter plots displaying the inverse Pearson correlation between DNA methylation value (*x*-axis) and *ZFP36L1* mRNA expression (*y*-axis) in bladder carcinoma. The probe ID is indicated on the top of each plot. PCC, Pearson correlation coefficient.

MutSig CV suggested that *ZFP36L1* was one of the prominently mutated drivers in bladder and breast cancers (Supplementary Fig. S1B). The Q value of false discovery rate of *ZFP36L1* was comparable with other well-known oncogenic drivers, such as *RB1* and *TP53*, implicating a potential tumor-suppressive role of *ZFP36L1* in these two types of cancer. mRNA expression of *ZFP36L1* was examined in healthy controls as well as in breast and bladder cancer samples using the Gene Expression Omnibus (GEO) database (25). Significant downregulation of *ZFP36L1* mRNA was observed in several independent patient cohorts of bladder (**Fig. 1B**) and breast cancers

Downloaded from http://aacrjournals.org/cancerres/article-pdf/80/2/219/2796271/219.pdf by guest on 27 August 2022

(Supplementary Fig. S1C), as compared with their adjacent normal tissues.

We performed IHC staining to examine ZFP36L1 protein expression in cancer samples. Compared with the matched normal tissues, ZFP36L1 staining was consistently reduced in bladder transitional carcinoma (**Fig. 1C**) and breast invasive ductal carcinoma (Supplementary Fig. S2A–S2C). This reduction of *ZFP36L1* expression was associated with worse survival in patients with breast cancer (Supplementary Fig. S2D–S2G).

Downregulation of *ZFP36L1* expression may be caused by either deletion or DNA/histone methylation of the *ZFP36L1* locus. Analysis of Genome Identification of Significant Targets in Cancer (GISTIC) SNP-array database (26) revealed that 4 cases of bladder cancer harbored homozygous deletions of *ZFP36L1* loci (chromosome 14q24.1). Given that DNA methylation is another possible cause of gene downregulation, DNA methylation levels at *ZFP36L1* gene locus were analyzed using Infinium Human Methylation 450K data generated by TCGA (27). These datasets contained 411 primary bladder cancer samples (vs. 17 normal bladder samples) and 778 primary breast cancer samples (vs. 83 normal breast samples; Supplementary Figs. S3–S6). Surprisingly, instead of the promoter regions, heavy methylations were found in the second exon of *ZFP36L1* in a subset of patient samples. Importantly, methylation levels of these regions were inversely correlated with *ZFP36L1* expression in the corresponding tumor samples (**Fig. 1D**; Supplementary Figs. S4 and S6). This suggests that downregulation of *ZFP36L1* in bladder and breast cancers were often caused by DNA methylation.

ZFP36L1 suppresses cell proliferation and migration

To test the functional importance of observed aberrant *ZFP36L1* expression, *ZFP36L1* was constitutively overexpressed (*CMV-ZFP36L1*) in several cell lines derived from muscle-invasive bladder cancer (J82, UMUC3 and HT1376) and breast cancer cell lines [HS578T (triple-negative), BT474 (ER^+, PR^+, $Her2^+$)]. Overexpression of *ZFP36L1* was confirmed using Western blot analysis (**Fig. 2A**). We examined *ZFP36L1* expression level in various bladder cancer cell lines, using RNA-sequencing data from Cancer Cell Line Encyclopedia. J82 had the lowest expression of *ZFP36L1*; therefore, it was selected as the model for overexpression. To identify the direct downstream targets of ZFP36L1, we also generated doxycycline-inducible *ZFP36L1*-overexpressing cells (*Tet-ZFP36L1*; Supplementary Fig. S7A–S7C).

We explored the effect of *ZFP36L1* on cell growth. Forced expression of *ZFP36L1* markedly impeded the proliferation of bladder and breast cancer cells (both constitutively expressed *CMV-ZFP36L1* and inducible *Tet-ZFP36L1*) in MTT assays (**Fig. 2A** and **B**; Supplementary Fig. S7D and S7E). To test the functional importance of RNA-recognizing motifs, two lentiviral *ZFP36L1*-mutant–expressing constructs were generated: (i) mutations of eight conserved Cysteine and Histidine amino acids in the CCCH arms of zinc-fingers to Alanine (namely ZFP36L1-Ala); (ii) deletions of two CCCH arms of ZFP36L1 (namely ZFP36L1-Del-CCCH). Forced expression of wild-type *ZFP36L1* suppressed foci formation of J82 and UMUC3 cells. Meanwhile, mutations of CCCH arms (Ala and Del CCCH) abolished the tumor-suppressive effect of *ZFP36L1*. Foci formation abilities of these mutant-transduced cells were similar to the control cells (**Fig. 2C** and **D**; Supplementary Fig. S7F and S7G). Forced expression of *ZFP36L1* also dramatically reduced colony formation of these cancer cells (**Fig. 2E**).

The effect of *ZFP36L1* on cell motility in bladder cancer cells was examined. Compared with J82 control cells, *ZFP36L1*-overexpressing cells had less ability to migrate. Western blots were performed to examine the expression of cell motility–related genes, and the results showed that vimentin and N-cadherin (two key regulators involved in cell adhesion and migration) were decreased in *ZFP36L1*-expressing cells (**Fig. 2F** and **G**; Supplementary Fig. S7H and S7I).

To explore the knockdown effect of *ZFP36L1* on cell growth, *ZFP36L1* was silenced using either CRISPR-Cas9 sgRNAs or siRNAs. As shown by Sanger Sequencing, CRISPR-Cas9 led to an indel in *ZFP36L1* gene locus in knockout cells (Supplementary Fig. S8). Western blot analyses demonstrated that ZFP36L1 was downregulated in cells transduced with either various sgRNAs or siRNAs. Silencing of *ZFP36L1* mildly enhanced cell growth and foci formation of bladder cancer cells (Supplementary Fig. S9A–S9C).

To investigate the inhibitory effect of *ZFP36L1* on tumorigenesis *in vivo*, either *ZFP36L1* knockdown T24, constitutive *CMV-ZFP36L1*–expressing HS578T, or *Tet-ZFP36L1*–expressing J82 and UMUC3 cells were injected subcutaneously into both flanks of immunodeficient NSG mice (**Fig. 2H**; Supplementary Fig. S9D–S9G). We explored the knockdown effect of *ZFP36L1 in vivo*. Depletion of *ZFP36L1* significantly enhanced tumor growth (Supplementary Fig. S9D). Elevation of *ZFP36L1* expression in the grafted tumors of *ZFP36L1*-overexpressing cells was confirmed by real-time PCR (Supplementary Fig. S9E). Tumor sizes were remarkably reduced or even completely absent in *ZFP36L1*-expressing cells, as compared with their controls in all experiments. Neither doxycycline-administered mice bearing control cells nor saline-treated mice bearing *Tet-ZFP36L1* cells (without doxycycline) had a significant effect on tumor size. Overall, these results demonstrate that *ZFP36L1* impairs tumor growth *in vivo*.

ZFP36L1 regulates pathways involved in inflammation, cell cycle, and hypoxic/HIF1A signaling

We initially attempted to perform RNA immunoprecipitation and sequencing (RIP-seq) to identify the binding targets of ZFP36L1. However, we failed to pull-down ZFP36L1 protein after trying several commercially available antibodies targeting human ZFP36L1. To address this issue, the concept of GST pull-down assay was adopted, using either wild-type (GST-ZFP36L1) or zinc-fingers mutant of ZFP36L1 (GST-ZFP36L1-Ala; **Fig. 3A**) fused with GST in its N-terminal, to pull-down cellular RNA. Affinity-purified recombinant proteins (either GST alone, GST-ZFP36L1, or GST-ZFP36L1-Ala) were incubated with nondenatured lysate of J82 cells to pull down the interacting RNA. The captured RNA was coprecipitated with the GST-recombinant proteins, purified with TRIzol and sequenced using high-throughput RNA-seq (**Fig. 3B**). Sequence analyses revealed a significant enrichment of ARE-containing transcripts, with AUUUA pentamers and UUAUUUAUU nonamers present in 96.4% and 14.8% of ZFP36L1-bound RNA, respectively (**Fig. 3C**). Further analyses of the 3′UTR regions of ZFP36L1-captured RNA sequences revealed several potential consensus recognition motifs, which included the canonical ARE sequence ($P = 1e^{-46}$). Analyses of sequencing results showed that the majority of the ZFP36L1-captured RNA encoded for functional proteins; less than 2% of them coded for pseudogenes and long noncoding RNAs (**Fig. 3D**).

To gain a better insight into ZFP36L1-regulated gene expression, transcriptome sequencing was performed to compare alterations of RNA transcripts before and after doxycycline-induced *ZFP36L1* expression (6 and 24 hours). A total of 4,147 differentially expressed ($\log_2 \geq 0.5$) transcripts were identified after 6 hours of doxycycline treatment, including 1,471 upregulated and 2,676 downregulated transcripts in *Tet-ZFP36L1*–expressing J82 bladder cancer cells. At 24 hours following doxycycline treatment, 2,864 upregulated and

Downloaded from http://aacrjournals.org/cancerres/article-pdf/80/2/219/2796271/219.pdf by guest on 27 August 2022

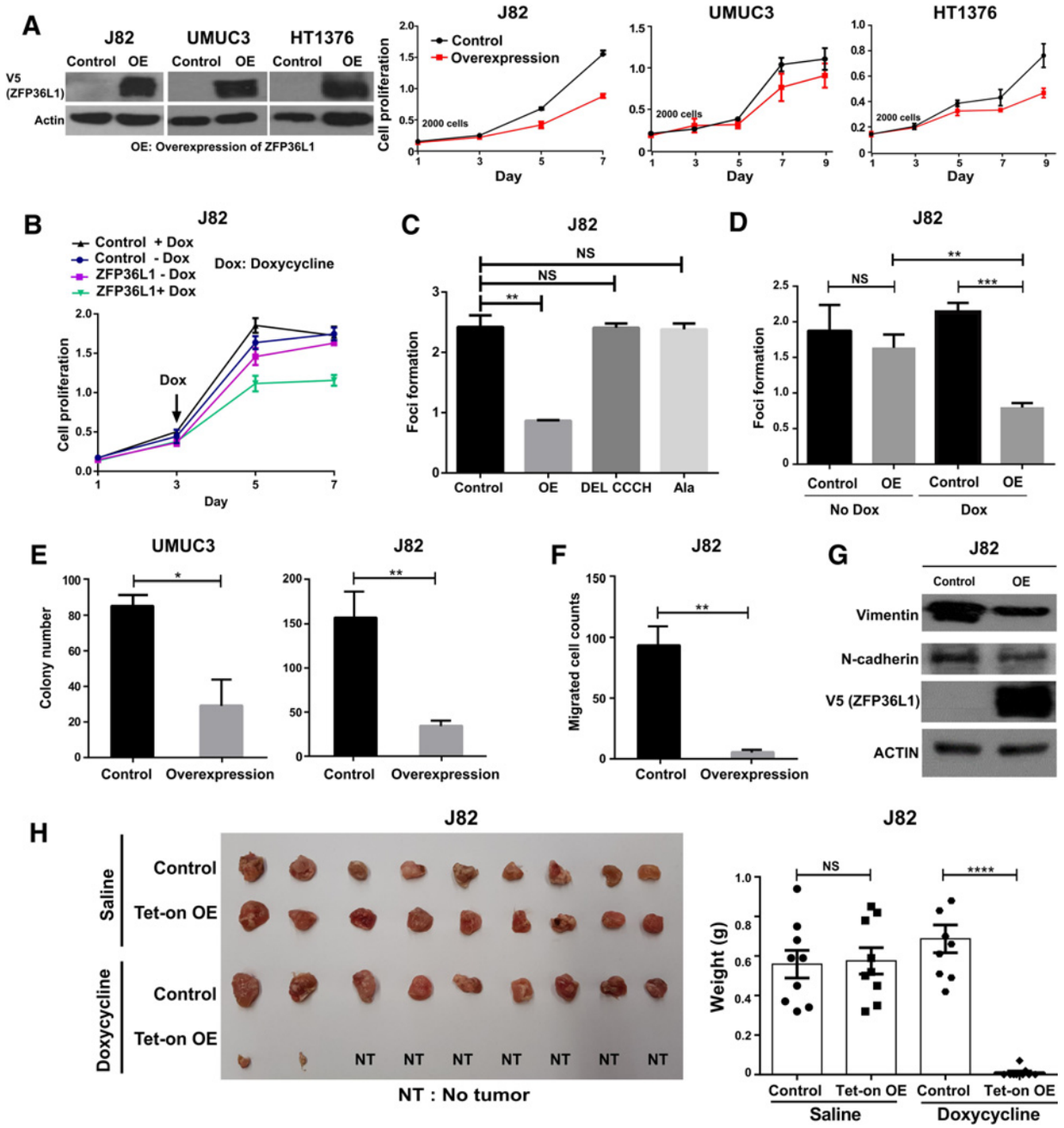

Figure 2.

ZFP36L1 suppresses proliferation, cell motility, and *in vivo* tumor growth. **A,** Left, representative Western blots of overexpression of V5-tagged ZFP36L1 in bladder cancer cell lines (J82, UMUC3, and HT1376). Right, MTT assays of J82, UMUC3, and HT1376 cells. Mean ± SD, $n = 6$. OE, overexpression of *ZFP36L1* (*CMV-ZFP36L1*). **B,** MTT assays of Tet-control (empty vector) or *Tet-ZFP36L1*–expressing J82 cells, growing either with or without doxycycline (Dox, 1 μg/mL). Mean ± SD, $n = 6$. **C** and **D,** Foci of J82 cells with *ZFP36L1* overexpression [wild-type (OE) or two *ZFP36L1* loss-of-function mutants (Del CCCH and Ala); **C**] and doxycycline (1 μg/mL)-induced *ZFP36L1*-expressing (with or without doxycycline) were grown for 3 weeks until the foci were visible (**D**). The foci were stained, dissolved with MTT stop solution, and measured using a spectrophotometer (O.D. 570). Mean ± SD, $n = 3$. **, $P < 0.01$; ***, $P < 0.001$. **E,** Forced expression of *ZFP36L1* (*CMV-ZFP36L1*) suppressed anchorage-independent growth of J82 and UMUC3 cells (5,000 cells per plate). Cells were grown in soft agar for a month. Colonies were stained and counted. Mean ± SD, $n = 3$. *, $P < 0.05$; **, $P < 0.01$. **F,** Forced expression of *ZFP36L1* (*CMV-ZFP36L1*) suppressed migration of J82 cells in Transwell assays (50,000 cells per well). Mean ± SD, $n = 3$. **, $P < 0.01$. **G,** Representative Western blots of expression of epithelial–mesenchymal transition markers in J82 cells. Forced expression of *ZFP36L1* (*CMV-ZFP36L1*) was detected using V5 antibody. β-Actin acted as a loading control. **H,** *ZFP36L1* suppressed the growth of bladder tumors *in vivo*. *Tet-ZFP36L1*–expressing or control J82 cells (1×10^6 cells) were resuspended in 100 μL FBS mixed with 100 μL Matrigel and injected subcutaneously into both flanks of immunodeficient NSG mice. Oral gavage of either saline (top rows) or doxycycline (bottom rows) was given to the mice every 4 days. Mice were sacrificed. Tumors were dissected, photographed (left), and weighed (right). NT, did not form tumors. Mean ± SD, $n = 9$. ****, $P < 0.0001$; NS, nonsignificant.

Downloaded from http://aacrjournals.org/cancerres/article-pdf/80/2/219/2796271/219.pdf by guest on 27 August 2022

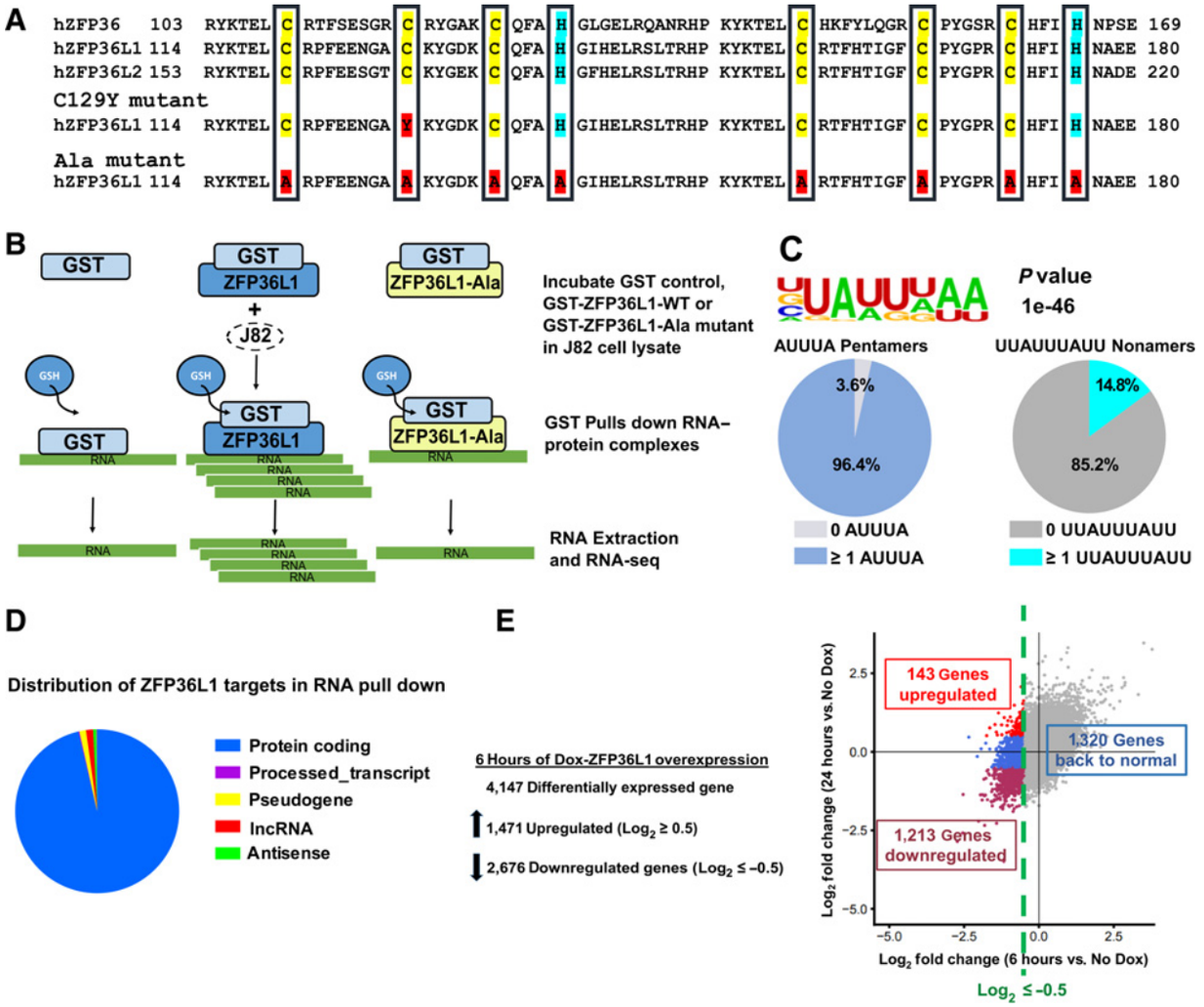

Figure 3.

RNA pull-down and RNA-seq using either wild-type or mutant ZFP36L1. **A,** Multiple sequence alignments of amino acid sequences of human ZFP36, ZFP36L1, ZFP36L2, and the mutants of ZFP36L1 generated in this study. **B,** The schematic diagram depicts the procedures of RNA pull-down experiments. Purified GST recombinant proteins (either GST alone, GST-ZFP36L1, or GST-ZFP36L1-Ala mutant) were incubated with total nondenatured cellular lysate of J82 for 2 hours at 4°C. Protein–RNA interaction complexes were captured by glutathione sepharose (GSH) beads. The pulled-down RNA was purified using TRIzol and profiled with high-throughput RNA-seq. **C,** AUUUA motifs were prominent in the 3′UTRs of RNA pulled down by GST-ZFP36L1, but neither by GST control nor GST-ZFP36L1-Ala–mutant protein. **D,** Distribution of ZFP36L1 targets in RNA pull-down experiments. **E,** Tightly regulated posttranscriptional regulation in J82 cells. Left, number of genes differentially expressed after 6 hours of doxycycline in *Tet-ZFP36L1*-expressing cells. Right, comparison of differentially expressed genes between 6 hours versus 24 hours of *Tet-ZFP36L1* expression.

1,847 downregulated transcripts were identified. The different patterns of gene alterations at 6 hours (early response genes) versus 24 hours (late response genes) following doxycycline induction may reflect the different layers of posttranscriptional regulation through ZFP36L1. For example, 2,676 genes that were downregulated at 6 hours displayed three different alterations at 24 hours after induction of ZFP36L1 expression: (i) continued to be downregulated (1,213 genes); (ii) returned to basal level (1,320 genes); or (iii) even slightly elevated (143 genes; **Fig. 3E**). Comparison of 6 hours versus 24 hours suggested a possible feedback mechanism in regulating some labile RNA to reverse the effect of *ZFP36L1* expression and dynamically maintaining the transcript levels of certain essential genes. The presence of such delicate mechanism may enable the cells to quickly respond to different signaling. Because many proto-oncogenes code for short-lived transcripts, we mainly focused on genes downregulated after 6 hours of doxycycline exposure.

To identify the direct downstream targets of ZFP36L1, a Venn diagram was generated with following criteria: (i) transcripts downregulated following 6 hours of doxycycline-induced *ZFP36L1* expression (2,676 genes), (ii) transcripts enriched in RNA pull-down experiments by GST-ZFP36L1, but not by the GST control (5,163 genes), (iii) transcripts containing WWAUUUAWW motifs in their 3′UTRs (15,317 genes). Following these criteria, we identified 1,410 direct downstream targets of ZFP36L1 (**Fig. 4A**; Supplementary Table S2). Gene ontology analyses of these 1,410 genes suggested an over-representation of genes involved in the cell cycle, proliferation,

Downloaded from http://aacrjournals.org/cancerres/article-pdf/80/2/219/2796271/219.pdf by guest on 27 August 2022

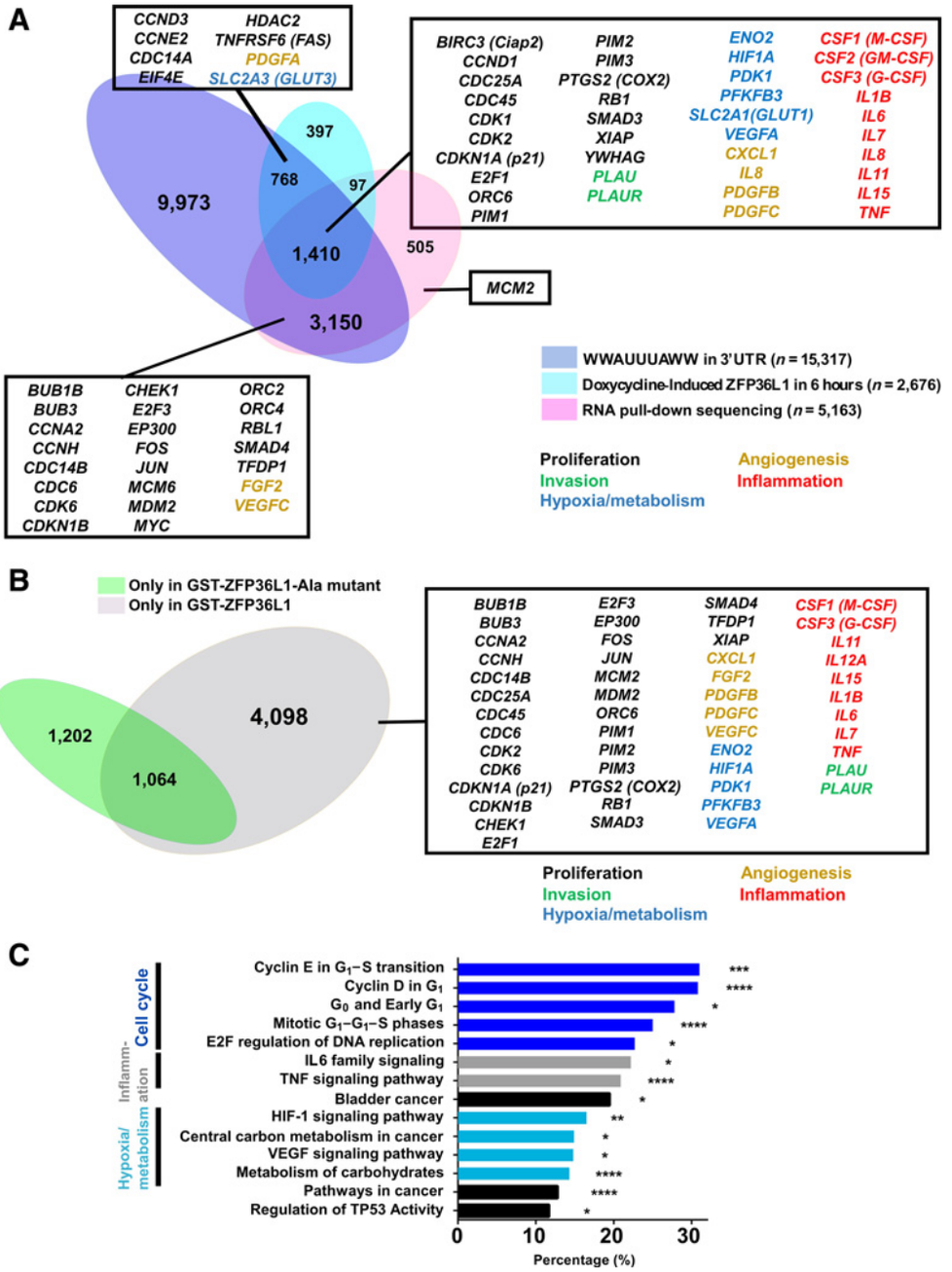

Figure 4.

Identification of ZFP36L1 direct targets using Venn diagrams analyses. **A,** Venn diagram of cancer-related RNAs showing the overlaps between: (i) RNA with WWAUUUAWW motifs in their 3′UTRs; (ii) RNA downregulated in the 6 hours of doxycycline-induced *ZFP36L1* overexpressing J82 cells, relative to *ZFP36L1* overexpressing cells without doxycycline induction; (iii) RNA bound by GST-ZFP36L1, but not GST control protein in RNA pull-down assay. The number of genes in each subset is indicated. These cancer-related RNAs are comprised of genes that are involved in proliferation, angiogenesis, hypoxia/metabolism, inflammation, and invasion. **B,** Venn diagram of cancer-related RNAs demonstrating the overlap between (i) RNA enriched by GST-ZFP36L1 versus GST control ($\log_2 \geq 0.5$) and (ii) RNA enriched by GST-ZFP36L1-Ala versus GST control ($\log_2 \geq 0.5$) in RNA pull-down assay. The number of genes in each subset is indicated. These cancer-related transcripts are comprised of genes involved in proliferation, angiogenesis, hypoxia/metabolism, inflammation, and invasion. **C,** Pathway enrichment analyses of 1,410 downstream targets of ZFP36L1 based on Venn diagram in **A** using KEGG and Reactome databases. Significantly enriched pathways are presented according to percentages of potential direct targets of ZFP36L1 compared with overall gene set. *, $P < 0.05$; **, $P < 0.01$; ***, $P < 0.001$; ****, $P < 0.0001$.

Downloaded from http://aacrjournals.org/cancerres/article-pdf/80/2/219/2796271/219.pdf by guest on 27 August 2022

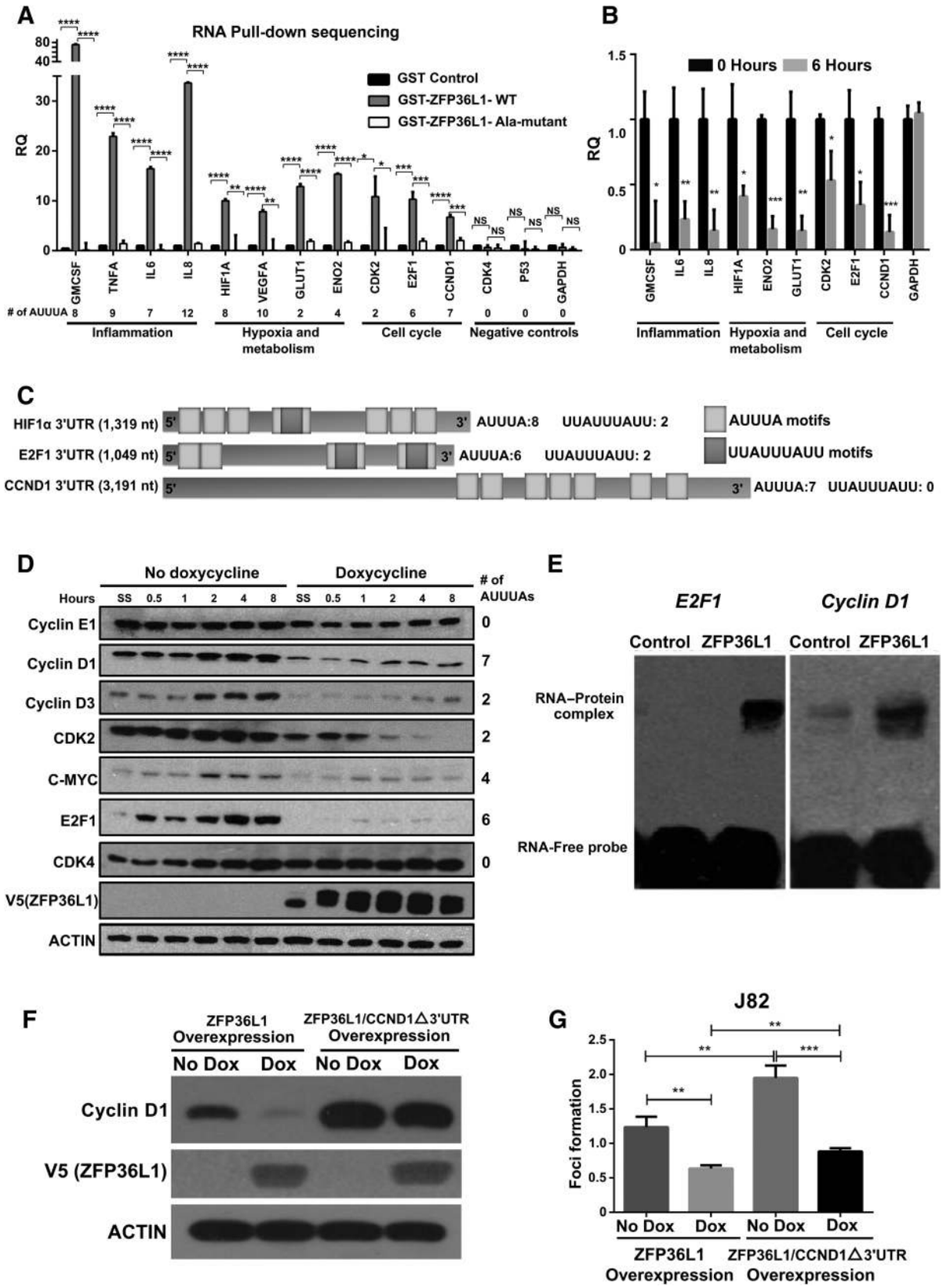

Downloaded from http://aacrjournals.org/cancerres/article-pdf/80/2/219/2796271/219.pdf by guest on 27 August 2022

inflammation, carcinogenesis, carbohydrate metabolism, and hypoxic signaling pathways. This was also validated by the Venn diagram of our pull-down assay, where only GST-ZFP36L1 was able to pull down many cancer-related genes (**Fig. 4B** and **C**), reinforcing the concept that zinc-finger CCCH arms of ZFP36L1 are required for recognition for of its RNA targets.

We also performed transcriptomic analyses of J82 knockdown cells and generated a Venn diagram with below criteria: (i) transcripts that were downregulated following 6 hours of doxycycline-induced *ZFP36L1* expression (2,676 genes); (ii) transcripts that were upregulated in *ZFP36L1* siRNA knockdown (1,646 genes); (iii) transcripts containing WWAUUUAWW motifs in their 3′UTRs (15,317 genes). Following these criteria, we identified 355 direct downstream targets of ZFP36L1 (Supplementary Fig. S10A). Gene ontology analyses of these commonly altered genes ($n = 355$) suggested an over-representation of genes involved in the cell cycle, inflammation, carbohydrate metabolism, and hypoxic signaling pathway (Supplementary Fig. S10B). These results were consistent with our findings (**Fig. 4**) and again supported the notion that ZFP36L1 is crucial in regulating inflammation, cell cycle, and hypoxia/*HIF1A* pathways in bladder cancer.

A number of selected genes were further validated using independent RNA pull-down experiments. For example, transcripts of *IL6* and *IL8* (inflammation pathway); *HIF1A, ENO2, GLUT1*, and *VEGFA* (hypoxic signaling); *CDK2, E2F1*, and *CCND1* (cell-cycle regulation); all have AUUUA motifs in their 3′UTRs and were significantly enriched by GST-ZFP36L1 recombinant protein (**Fig. 5A**). The ZFP36L1 RNA pull-down experiments appeared to be highly specific for AUUUA-containing transcripts, as highly expressed transcripts without 3′UTR ARE sites (such as *GAPDH, CDK4* and *TP53*) were not captured. Consistently, RT-PCR analyses indicated that the RNA levels of the aforementioned ZFP36L1 downstream targets were quickly and profoundly decreased following doxycycline (6 hours), compared with the untreated control cells (0 hour; **Fig. 5B**). Collectively, these data highlight a sequence-specific ZFP36L1-mediated transcriptome regulatory circuit in recognizing and mediating ARE-containing RNA degradation.

ZFP36L1 suppresses the expression of key cell-cycle regulators

Three procancer genes (*E2F1, CCND1, HIF1A*) were selected for further investigation. These genes comprise a number of AUUUA motifs with different classes of ARE in their 3′UTRs (**Fig. 5C**). E2F1 and CCND1 are two critical cell-cycle regulators. The binding and downregulation of both gene transcripts by ZFP36L1 suggested the latter might play a crucial role in the regulation of cell-cycle progression. Indeed, gene set enrichment analyses (GSEA) of RNA-seq in TCGA data showed that bladder tumor samples that had high *ZFP36L1* expression displayed a lower expression of hypoxic and cell-cycle–related genes, whereas those with low *ZFP36L1* expression displayed an elevated expression of ARE-containing cell-cycle genes (Supplementary Fig. S11A–S11C). Our analyses were extended to a number of crucial cyclins (CCN), cyclin-dependent kinases (CDK), and other key cell-cycle regulators, including cyclin D1, cyclin D3, c-MYC, E2F1, and CDK2 (**Fig. 5D**; Supplementary Figs. S11D, S12A, and S12B). Protein levels of these cell-cycle regulators were elevated by serum-stimulation in a time-dependent manner; and these elevations were consistently abrogated by doxycycline-induced ZFP36L1 expression. Conversely, protein levels of non-ARE cell-cycle regulators such as cyclin E1 and CDK4 remained unaffected. Similar results were also observed in T24 bladder cancer cells, whereby cell-cycle regulators, such as cyclin D1 and E2F1, were upregulated in *ZFP36L1* knockdown cells. Overall, this underscores the selective regulation of ZFP36L1 on ARE-containing cell-cycle regulators.

To demonstrate that ZFP36L1 suppresses these cell-cycle regulators by directly binding to their 3′UTR ARE motifs, RNA-EMSA was performed to examine the protein–RNA interaction. The 3′UTRs of *CCND1* and *E2F1* contain 7 AUUUA pentamers, and 6 AUUUA pentamers as well as 2 nonamers, respectively (**Fig. 5C**). Biotinylated RNA probes containing the AREs sequences were designed on the basis of either *E2F1* or *CCND1* 3′UTR (Supplementary Table S3) and were synthesized using T7 *in vitro* transcription. The purified RNA probes were incubated with cellular protein lysates of either *ZFP36L1* or control plasmid overexpression. A "gel shift" band was readily observed in the lanes containing lysates of cells overexpressing *ZFP36L1*, confirming a direct interaction between ZFP36L1 and ARE-containing RNA sequences (**Fig. 5E**).

Rescue experiments were performed using *CCND1* overexpression construct without its 3′UTR (*CCND1*△3′UTR) in *Tet-ZFP36L1*–expressing cells. Cells transduced with this construct successfully rescued CCND1 protein expression (**Fig. 5F**), and partially abolished the growth-suppressive effect of *ZFP36L1* (**Fig. 5G**). This observation suggested that CCND1 functions as a direct downstream effector of ZFP36L1. Nevertheless, forced expression of *CCND1* was insufficient

Downloaded from http://aacrjournals.org/cancerres/article-pdf/80/2/219/2796271/219.pdf by guest on 27 August 2022

Figure 5.

ZFP36L1 regulates pathways of the cell cycle, inflammation, and hypoxic signaling. **A,** Real-time PCR to validate the candidate targets pulled down by GST-ZFP36L1, but not by either GST control or GST-ZFP36L1-Ala mutant. Transcripts that do not contain AUUUA motifs in their 3′UTR (*CDK4, TP53*, and *GAPDH*) served as negative controls. RQ, relative quantification of RNA, which was normalized on the basis of GST control. The number of AUUUA motifs (# of AUUUA) found in their respective 3′UTR are listed below the gene names. **B,** Downstream targets of ZFP36L1 were downregulated after doxycycline-induced *ZFP36L1* overexpression. *Tet-ZFP36L1*–expressing J82 cells were treated with doxycycline for 6 hours to induce *ZFP36L1* expression. RT-PCR validated alterations of expression of indicated genes. *GAPDH* served as a negative control. **C,** Diagram depicts ARE sites in 3′UTR regions of *HIF1A, CCND1* and *E2F1.* Light gray, AUUUA motifs; dark gray, UUAUUUAA motifs. The number of AUUUA motifs are indicated. **D,** ZFP36L1 suppressed the expression of ARE-containing cell-cycle regulators. *Tet-ZFP36L1*-expressing J82 cells (with or without doxycycline) were serum-starved (SS) to synchronize cells to G_0 stage and were serum-stimulated to promote cell-cycle progression. Protein lysates were collected at different time points. Western blot analyses were performed to detect alterations of cell-cycle–related proteins. ZFP36L1 overexpression was detected using V5 antibody. The number of AUUUA motifs (# of AUUUAs) in the 3′UTR of each corresponding gene is indicated on the right side. Each experiment was repeated three times and a representative result is shown. **E,** ZFP36L1 bound to RNA probes derived from the sequences of *cyclin D1* or *E2F1* 3′UTR. RNA-EMSA was performed by incubating biotinylated RNA probes (corresponding to sequences containing pentameric or nonameric AUUUA sequences of either *CCND1* or *E2F1* 3′UTR), with protein lysates of cells transfected either with control vector or *ZFP36L1* expression construct. Full sequence of *E2F1* RNA probe is CCAGCCTGTTTGGAAAC**ATTTAATTTA**TACCCC and full sequence of *CCND1* RNA probe is CAGTATG**ATTTA**TAAATGCAATCTCCCCTTG**ATTTA**AAC (ATTTA motifs are underlined). **F,** Overexpression of *CCND1* without 3′UTR (*CCND1*△3′UTR) restored CCND1 protein expression in *Tet-ZFP36L1* J82 cells. Western blot analyses were performed to examine CCND1 and ZFP36L1-V5 expression. ZFP36L1 overexpression was detected using V5 antibody. Each experiment was repeated three times and a representative result is shown. **G,** Overexpression of *CCND1* partially rescued suppressive effect of *ZFP36L1* of growth of bladder cancer cells. Foci of *Tet-ZFP36L1* or control J82 cells [with or without doxycycline (Dox), 1 μg/mL] were grown for 3 weeks until the foci were visible and were stained. Foci were dissolved with MTT stop solution and were measured using spectrophotometer (O.D., 570). Mean ± SD, $n = 3$. *, $P < 0.05$; **, $P < 0.01$; ***, $P < 0.001$; ****, $P < 0.0001$.

to reverse the growth-suppressive effect of *ZFP36L1*, suggesting that apart from *CCND1*, other downstream effectors (e.g., other cell-cycle regulators) also contribute to the tumor-suppressive effect of ZFP36L1.

ZFP36L1 regulates the hypoxic/*HIF1A* signaling

HIF1A is another key downstream target of ZFP36L1. Doxycycline-induced *ZFP36L1* expression suppressed the expression of HIF1A at both protein and mRNA levels (**Fig. 6A–C**; Supplementary Fig. S12C). Meanwhile, silencing of *ZFP36L1* leads to a significant upregulation of *HIF1A* in both normoxic and hypoxic conditions (Supplementary Fig. S12D). These results suggested that ZFP36L1 is a crucial destabilizing factor of *HIF1A*. HIF1A is the central regulator of hypoxic signaling and it transactivates many downstream genes involved in angiogenesis and glucose metabolism. As expected, suppression of *HIF1A* expression by *ZFP36L1* downregulated HIF1A downstream targets, such as lactate dehydrogenase (*LDHA*). Given that the 3′UTR of *LDHA* does not contain AUUUA motifs, the significant downregulation of *LDHA* mRNA that we observed in *ZFP36L1*-expressing cells was likely due to the downregulation of its upstream transcription activator, *HIF1A*. To test whether enforced expression of *ZFP36L1* leads to aberrant glycolysis, the lactate concentration of the conditioned media of cells ± *ZFP36L1* was measured. In line with the downregulation of expression of *HIF1A, LDHA*, and *PDK1* (key glycolysis enzymes), less lactate (the end product of glycolysis) was detected (**Fig. 6D** and **E**). Dysregulated metabolic reprogramming, such as aberrant glycolysis and increased glucose uptake, is a metabolic hallmark of cancers. Importantly, ZFP36L1 not only suppressed mRNA stability of *HIF1A*, but also directly recognized and suppressed the expression of a number of HIF1A downstream genes involved in the glycolytic pathway, such as glucose transporter (*GLUT1/SLC2A1*), enolase 2 (*ENO2*), phosphoinositide-dependent kinase 1 (*PDK1*), and *VEGFA*. This conclusion was supported by (i) each of these transcripts involved in glycolytic pathways contains AUUUA motifs in their 3′UTRs; (ii) forced expression of *ZFP36L1* decreased their RNA levels (**Fig. 6E**); (iii) these transcripts were specifically pulled down by GST-ZFP36L1 protein (Supplementary Table S2). Interestingly, forced expression of *HIF1A* reciprocally reduced ZFP36L1 mRNA and protein expression (Supplementary Fig. S12E), suggesting that a feedback interplay may occur between *HIF1A* signaling and *ZFP36L1* expression. Collectively, our observations suggest a critical role of *ZFP36L1* in hypoxia-regulated glucose metabolism process. As such, loss of *ZFP36L1* expression may result in a dysfunctional cellular metabolic program that promotes bladder tumorigenesis.

Previous research has suggested that ZFP36L1 is involved in regulating vascularization by destabilizing *VEGFA* mRNA (23), which is also a key downstream effector of HIF1A. Indeed, *VEGFA* mRNA level was significantly decreased upon *ZFP36L1* forced expression (**Fig. 6E**). Congruently, enlarged tumor size (Supplementary Fig. S12F) and increased vascular formation (Supplementary Fig. S12G) occurred after silencing *ZFP36L1* in chorioallantoic membrane assay. These data suggest that *ZFP36L1* contributes to the regulation of tumor angiogenesis, by negatively modulating angiogenic factors including *VEGFA* expression.

ZFP36L1 binds to *HIF1A* 3′UTR and promotes its mRNA degradation

The 3′UTR of *HIF1A* contains eight pentamers (AUUUA) and one nonamer (UUAUUUAUU) of the ARE motifs (**Fig. 5C**), which serve as potential binding targets for ZFP36L1. To demonstrate that ZFP36L1 mediates *HIF1A* mRNA degradation via ARE motifs in its 3′UTR, dual-luciferase assays were performed using *Renilla-PEST* reporter gene fused to the entire 3′UTR sequence of *HIF1A* (**Fig. 7A**). The *PEST* domain, which is fused with a *Renilla luciferase* gene, facilitates protein degradation and prevents protein accumulation of *Renilla* luciferase (half-life < 2 hours), thus providing a sensitive technique to measure the amount of RNA present. The reporter plasmid was cotransfected with either *ZFP36L1* or control plasmid into HEK293T cells. The amount of transcript of *Renilla-HIF1A* 3′UTR was inferred on the basis of the level of *Renilla* luciferase activity. Forced expression of *ZFP36L1* profoundly reduced *Renilla* activity in a dose-dependent manner (**Fig. 7B**), indicating that ZFP36L1 regulates *HIF1A* mRNA decay through its ARE-containing 3′UTR.

Next, we asked whether the integrity of the zinc-finger arms of ZFP36L1 is required for the degradation of *HIF1A* mRNA. Two mutants of ZFP36L1 were generated: (i) ZFP36L1-C129Y, a missense mutant found in breast carcinoma sample (TCGA-A8-A084-01); (ii) ZFP36L1-Ala (**Fig. 3A**). Dual-luciferase assays were performed by cotransfecting *Renilla-HIF1A* 3′UTR reporter plasmid together with wild-type *ZFP36L1* and two *ZFP36L1* mutants' plasmids. Results indicated that the ZFP36L1-C129Y mutant partially retained the suppressive activity, albeit to a lesser extent as compared with wild-type ZFP36L1 (**Fig. 7B**). In contrast, ZFP36L1-Ala mutant completely abolished the ZFP36L1-mediated *Renilla-HIF1A* 3′UTR RNA decay, suggesting that the intact zinc-finger arms are critical for ZFP36L1-mediated RNA decay.

To investigate whether the number of AUUUA motifs affect the binding affinity and RNA degradation of ZFP36L1, several constructs were generated using the same *Renilla-PEST* reporter plasmid (**Fig. 7A**) with different numbers of AUUUA motifs, based on the sequences of *HIF1A* 3′UTR (**Fig. 7C** and **D**). ZFP36L1 significantly suppressed activities of *Renilla luciferase* gene fused with 3′UTR sequences of either AT1x, AT2x, AT3x, AT4x, or AT5x, but not with the negative controls (GC5x and AT2xT). The increasing number of AUUUAs in 3′UTR enhanced the efficiency of ZFP36L1-mediated RNA decay, whereby the *Renilla luciferase* gene fused with 5x AUUUAs (AT5x) motifs reduced *Renilla* activity mediated by ZFP36L1 to the greatest extent. A decrease of *Renilla* luciferase activity was also observed in the control cells, perhaps mediated by endogenous RNA-binding proteins.

To demonstrate the direct binding of ZFP36L1 to AUUUA motifs in *HIF1A* 3′UTR, RNA-EMSA experiments were performed. Gel mobility shift induced by ZFP36L1 binding was clearly observed with *HIF1A* 3′UTR RNA (**Fig. 7E**). Coincubation of nonbiotinylated *HIF1A* 3′UTR RNA probes (cold competitor, 1:500) abrogated ZFP36L1 binding, emphasizing the sequence specificity of this interaction (**Fig. 7F**). Collectively, these results strongly suggest that ZFP36L1 mediates *HIF1A* mRNA decay by specifically recognizing the AUUUA motifs in its 3′UTR.

Discussion

ZFP36L1 is a novel tumor suppressor involved in hypoxia, cell-cycle progression, angiogenesis, and metabolism. We found that it is often epigenetically silenced and downregulated in bladder and breast cancers (**Fig. 2**; Supplementary Figs. S2, S13, and S14). Interestingly, instead of epigenetic modifications of the promoter regions, heavy methylations were observed in the second exon of *ZFP36L1* (~2.5 kb downstream of the transcriptional start site, chr14:68789960-68790319) in a subset of patients. This region is often associated with a permissive enhancer mark (H3K27Ac). When we analyzed the potential enhancers/regulatory elements using H3K27Ac Chip-Seq

Downloaded from http://aacrjournals.org/cancerres/article-pdf/80/2/219/2796271/219.pdf by guest on 27 August 2022

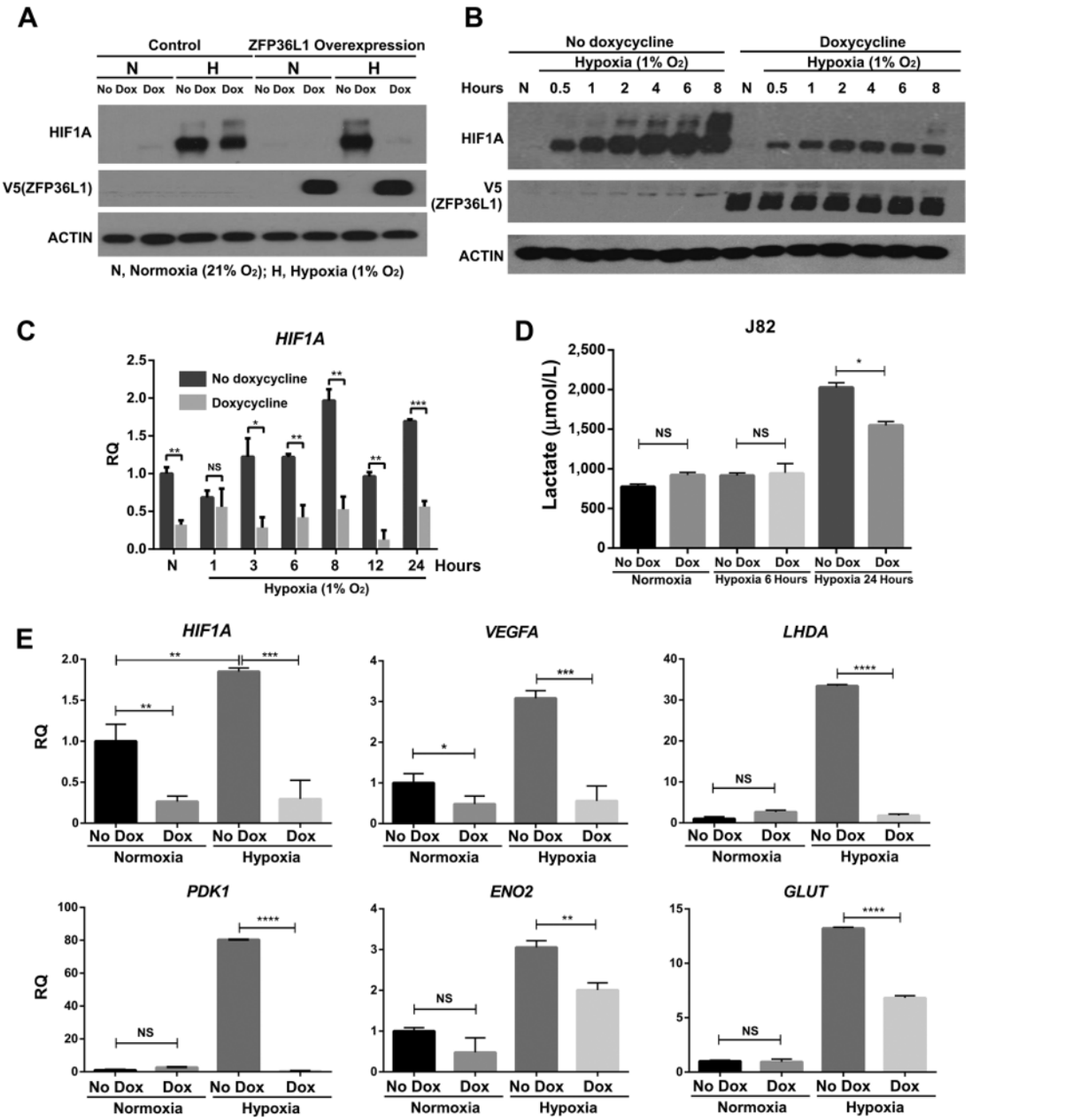

Figure 6.

ZFP36L1 downregulates the expression of HIF1A and its downstream targets. **A** and **B,** ZFP36L1 downregulated HIF1A protein expression. **A,** Representative Western blot analysis of doxycycline (Dox)-induced (1 μg/mL, 12 hours) expression of ZFP36L1. J82 cells were grown under normoxic (N, 21% oxygen) or hypoxic (H; 1% oxygen in a hypoxia chamber) for another 12 hours. Untransfected (control) J82 cells were subjected to the same condition. Each experiment was repeated three times and a representative result is shown. **B,** *Tet-ZFP36L1*-expressing J82 cells were treated either with or without doxycycline (1 μg/mL) for 12 hours to induce ZFP36L1 protein expression. Cells were then grown under either normoxic (N, 21% O_2) or hypoxic condition (1% O_2; same as below) for 0–8 hours. ZFP36L1 expression was detected using V5 antibody. β-Actin acted as a loading control. **C,** ZFP36L1 downregulated *HIF1A* mRNA expression. Real-time PCR was performed to examine *HIF1A* expression in *Tet-ZFP36L1*–expressing J82 cells, incubated either with or without doxycycline (1 μg/mL, 12 hours) to induce *ZFP36L1* expression prior to exposure to either normoxic or hypoxic condition for 0–24 hours. Mean ± SD, $n = 3$. **D,** ZFP36L1 reduced lactate production of J82 cell growth in hypoxia. *Tet-ZFP36L1*–expressing J82 cells were treated with doxycycline (1 μg/mL; 12 hours) to induce *ZFP36L1* expression and were grown in either normoxic or hypoxic condition for 6 hours and 24 hours. Level of lactate in the conditioned medium was determined by using the L-lactate assay kit. Mean ± SD, $n = 3$. **E,** ZFP36L1 downregulated the expression of HIF1A downstream targets. *Tet-ZFP36L1*–expressing J82 cells were treated either with or without doxycycline (1 μg/mL) for 12 hours and then placed under either normoxic or hypoxic conditions for 4 hours. Real-time PCR was performed to measure mRNA expression of *HIF1A, LDHA, GLUT3, VEGFA, ENO2*, and *PDK1*. Mean ± SD, $n = 3$. *, $P < 0.05$; **, $P < 0.01$; ***, $P < 0.001$; ****, $P < 0.0001$; NS, nonsignificant.

Downloaded from http://aacrjournals.org/cancerres/article-pdf/80/2/219/2796271/219.pdf by guest on 27 August 2022

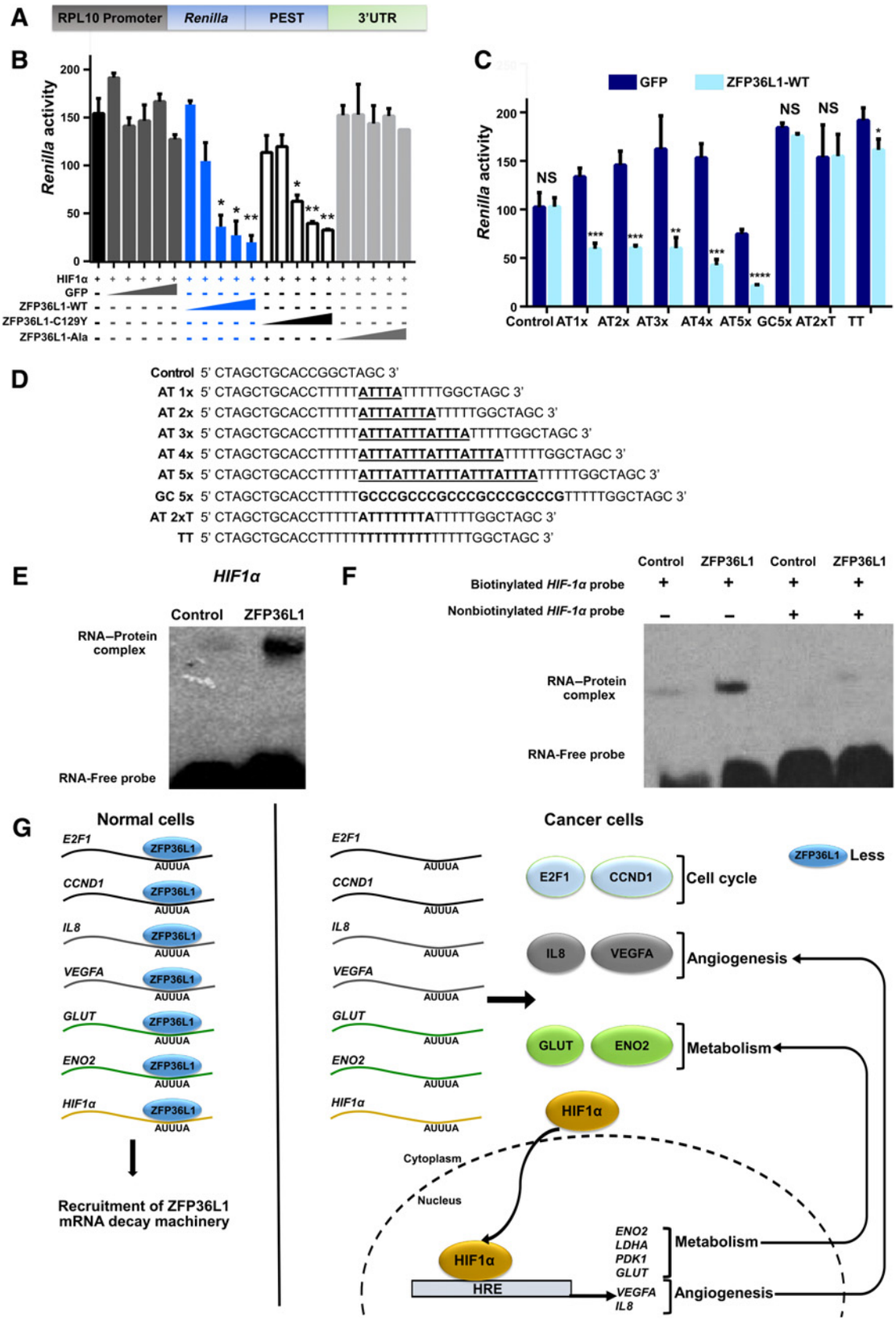

Downloaded from http://aacrjournals.org/cancerres/article-pdf/80/2/219/2796271/219.pdf by guest on 27 August 2022

data from ENCODE database (28), enrichments of H3K27Ac peaks in the second exon of *ZFP36L1* were observed in a variety of cells (normal and cancer cells), suggesting that an enhancer is located in that position probably to regulate *ZFP36L1* expression. Recent studies suggested that aberrant DNA methylation that occurs in regions beyond the CpG islands of promoter regions, such as distant enhancer or an enhancer inside the gene body, can silence the gene (29–32). Consistent with our findings, a recent study also suggested that *ZFP36L1* expression is silenced through elevated DNA methylation in the same exon 2 position in myelofibrosis (33). Interestingly, we recently showed a gain of DNA methylation of distant upstream of *ZFP36L2* prevented the formation of H3K27 super-enhancers, blunting the expression of *ZFP36L2* in esophageal squamous cell carcinoma samples (34). Analyses across different cancer types suggested that dynamic methylation patterns in the enhancer regions might be a frequent event during the malignant transformation and cancer progression (32).

Previous studies have suggested a functional redundancy that occurs between the three ZFP36 family members (18, 21, 35), due to their highly conserved tandem zinc-finger domains that recognize similar AUUUA motifs. Indeed, many targets of ZFP36 (e.g., *TNF, COX-2, IL6, IL8, cyclin D1, HIF1A, E2F1*, and *GM-CSF*) are also bound by ZFP36L1. In addition, functional redundancy has been proposed between ZFP36L1 and ZFP36L2 in a murine T-ALL model induced by double knockout of *Zfp36l1/l2*, whereby a single conditional knockout of either *Zfp36l1* or *Zfp36l2* fail to develop T-ALL (18). Nevertheless, studies have also suggested that each member of the ZFP36 family has its unique downstream targets (36), possibly due to the unique amino acid sequences in their C- and N-terminal regions. For example, in human Burkitt lymphoma, only *ZFP36*, but not *ZFP36L1*, is able to suppress MYC-induced lymphomagenesis (37). Furthermore, knockouts of different *Zfp36* family members in murine models have been shown to display distinct phenotypes. The *Zfp36*-deficient mice suffer from severe chronic inflammation due to the accumulation of *TNF-α* mRNA (38), while *Zfp36l1* homozygous knockout mice die on embryonic day 11, possibly as a consequence of chorioallantoic fusion failure (39). Mice with a homozygous knockout of *Zfp36l2* die within 2 weeks of birth due to hematopoietic stem cell failure (40). Interestingly, our RNA pull-down results suggested that ZFP36L1 also binds to the mRNA of its paralog, *ZFP36L2*. In line with this observation, doxycycline-induced expression of *ZFP36L1* downregulates *ZFP36L2* mRNA level. Congruently, a recent report shows that ZFP36L1 binds to *ZFP36L2* mRNA, and silencing of *ZFP36L1* is associated with an increased level of *ZFP36L2* mRNA in marginal-zone B cells (41). Taken together, these data suggest signaling crosstalk and functional overlap of these three family members in both normal and cancer cells.

Upregulation of key cell-cycle regulators *E2F1* and *cyclin D1* enhances the aggressiveness of bladder cancer, correlates with tumor recurrence and lymph node metastasis, and is associated with worse overall survival (42–44). In fact, amplification of *cyclin D1* and *E2F* family members are key molecular signatures to define different subtypes of bladder cancer (45). ZFP36L1 profoundly suppresses the expression of *E2F1* and *cyclin D1*, as well as a number of important cell-cycle regulators, such as *CDK2, cyclin D3*, and *c-MYC* (**Fig. 5B** and **D**), suggesting its critical role as a negative regulator in controlling cell-cycle progression. Recently, ZFP36L1 has been reported to drive monocyte/macrophage differentiation by negatively regulating *CDK6* (46), as well as control B lymphocytes and marginal zone B cells development by suppressing CDKs/cyclins and lineage transcription factors (*KLF2* and *IRF8*; refs. 41, 47). ZFP36L1 also controls thymic β-selection checkpoint, through limiting DNA damage response and expression of cell-cycle regulators (*CCND3* and *CCNE2*; ref. 35). A study from Suk and colleagues demonstrated that overexpression of *ZFP36L1* and *ZFP36L2* inhibits cellular proliferation of colorectal cancer cell lines by suppressing various cell-cycle–related proteins, such as cyclin A, cyclin B, cyclin D, and p21 (21). Consistent with their finding, we demonstrated that ZFP36L1 regulates cell-cycle progression by suppressing key cell-cycle regulators, including cyclin D1, cyclin D3, CDK2, c-MYC, and E2F1 (**Fig. 5D**). Truncating mutations or epigenetic downregulation of *ZFP36L1* in tumor samples might lead to aberrant upregulation of cell-cycle genes, and thus contributing to the progression of bladder cancer. Suk and colleagues also showed interesting data concerning overexpression of either *ZFP36L1* or *ZFP36L2* enhances wild-type TP53 protein expression. However, *TP53* does not have AUUUA motifs; and in our study, *TP53* mRNA was not pulled down by ZFP36L1. Hence, how the level of *TP53* might be regulated remains unknown. The increased level of TP53 protein might be due to a secondary effect of *ZFP36L1* overexpression, possibly by downregulation of *MDM2* (contains 22 AUUUA motifs in its 3′UTR) by ZFP36 family members. The potential

Figure 7.

ZFP36L1 binds to the 3′UTR of *HIF1A* mRNA and causes its degradation. **A,** The schematic diagram shows the *Renilla* reporter plasmid used in the study. *HIF1A* 3′UTR was placed downstream of *Renilla-PEST* gene, which was driven by a constitutive *RPL10* promoter. Hereafter, it is referred to as *Renilla-HIF1A* 3′UTR plasmid. *PEST* is a protein destabilization domain that reduces the protein half-life of *Renilla* luciferase. **B,** ZFP36L1 suppressed the expression of *Renilla-HIF1A* 3′UTR in a dose-dependent manner. *Renilla-HIF1A* 3′UTR reporter plasmid was cotransfected with different amount (μg) of control, *ZFP36L1* or mutants (*ZFP36L1-C129Y* or *ZFP36L1-Ala*) plasmids. *Renilla* luciferase activity was measured 24 hours posttransfection and was normalized with the cotransfected firefly luciferase (*CMV-Luc* plasmid) activity. Mean ± SD, $n = 3$. *, $P < 0.05$; **, $P < 0.01$. **C,** HEK293T cells were cotransfected with *Renilla luciferase* reporter plasmids containing different 3′UTR sequences as shown in **D**, together with either control or *ZFP36L1* overexpression plasmid. *Renilla* luciferase activity was measured 24 hours posttransfection and was normalized with cotransfected firefly luciferase (*CMV-Luc* plasmid) activity. Mean ± SD, $n = 3$. **, $P < 0.01$; ***, $P < 0.001$; ****, $P < 0.0001$; NS, nonsignificant. **D,** Different numbers of ATTTA (AUUUA RNA motifs, sequences modified from AT2x originally from *HIF1A* 3′UTR) were inserted into the 3′UTR regions of *RPL10-Renilla-PEST* plasmid (right after the stop codon of *Renilla luciferase* gene). In GC5x sequence, A and T deoxynucleotides were substituted with G and C deoxynucleotides, acting as a negative control of the experiment. AT2xT has a single point mutation of A to T deoxynucleotide to disrupt the AUUUA motif. TT was modified from AT2x by mutating all the A deoxynucleotides to T. **E,** ZFP36L1 bound to AUUUA motifs of *HIF1A* 3′UTR. RNA-EMSA was performed by incubating biotinylated RNA probes (corresponding to nucleotide sequences containing pentameric AUUUA sequence of *HIF1A* 3′UTR) with total protein lysates of HEK293T cells transfected with either control or *ZFP36L1* expression vector. Sequence of RNA probe is CTGTATGGTTTATT**ATTTA**AATGGGTAAAGCCATTTACA. ATTTA motif is underlined. Each experiment was repeated three times and a representative result is shown. **F,** Nonbiotinylated RNA probes of *HIF1A* competed for the binding of ZFP36L1 protein. RNA-EMSA was performed with incubation of biotinylated probes (2 nmol/L) ± competitive unbiotinylated RNA probes (1 μmol/L) of *HIF1A*, together with lysates from HEK293T cells transfected with either control or *ZFP36L1* expression construct. Each experiment was repeated three times and a representative result is shown. **G,** Schematic diagram summarizing the role of *ZFP36L1* in regulating posttranscriptional targets in cancer cells. In normal cells, ZFP36L1 acts as an adaptor protein to recruit RNA decay machinery. In cancer cells, ZFP36L1 is often either epigenetically silenced or mutated. Therefore, many of its downstream targets are upregulated at both the RNA and protein levels, contributing to cell cycle, angiogenesis, metabolism, and ultimately to tumorigenesis.

Downloaded from http://aacrjournals.org/cancerres/article-pdf/80/2/219/2796271/219.pdf by guest on 27 August 2022

relationships between *MDM2-TP53* and *ZFP36* family members deserve further investigation.

In summary, our study identifies a previously unappreciated tumor suppressor role of *ZFP36L1* in bladder and breast cancers and delineates a number of its downstream targets. We reveal that *ZFP36L1* is a posttranscriptional regulator of hypoxic adaptation, metabolism, angiogenesis, and cell-cycle progression in bladder cancer cells (**Fig. 7G**). Pharmacologic induction to enhance *ZFP36L1* expression should be explored as a potential therapeutic intervention for certain cancers.

Disclosure of Potential Conflicts of Interest

No potential conflicts of interest were disclosed.

Authors' Contributions

Conception and design: Q.-Y. Sun, L.-W. Ding, J.W. Said, H.P. Koeffler
Development of methodology: X.-Y. Loh, Q.-Y. Sun, L.-W. Ding, N. Venkatachalam, J.W. Said, A.P.-F. Koh
Acquisition of data (provided animals, acquired and managed patients, provided facilities, etc.): X.-Y. Loh, Q.-Y. Sun, L.-W. Ding, J.-F. Xiao, J.W. Said, P. Shyamsunder, A.P.-F. Koh, R.Y.-J. Huang
Analysis and interpretation of data (e.g., statistical analysis, biostatistics, computational analysis): X.-Y. Loh, Q.-Y. Sun, L.-W. Ding, A. Mayakonda, N. Venkatachalam, T.C. Silva, J.W. Said, X.-B. Ran, S.-Q. Zhou, P. Dakle, A.P.-F. Koh, B.P. Berman, H. Yang, D.-C. Lin
Writing, review, and/or revision of the manuscript: X.-Y. Loh, Q.-Y. Sun, L.-W. Ding, J.W. Said, S.-Q. Zhou, S.-Y. Tan, H.P. Koeffler
Administrative, technical, or material support (i.e., reporting or organizing data, constructing databases): M.-S. Yeo, N.B. Doan, A.P.-F. Koh
Study supervision: Q.-Y. Sun, L.-W. Ding, H.P. Koeffler

Acknowledgments

We thank Dr. Park Mi Kyoung for the generous sharing of the bladder cancer cell lines. We thank Dr. Professor Ronald Hay and Dr. John Bett for their generous sharing of vectors (*Renilla-PEST-HIF* reporter plasmids) as well as Dr. Xiaoyuan Wang and Dr. Jiong-Wei Wang for sharing experimental apparatus. We also thank Dr. Sudhakar Jha and Professor Lorenz Poellinger for their helpful advice, as well as Professor Harvey R. Herschman (a pioneer of this field), a friend and mentor of H.P. Koeffler. This research was supported by the National Research Foundation Singapore under Singapore Translational Research (STaR) Investigator Award (NMRC/STaR/0021/2014) and Singapore Ministry of Education Academic Research Fund Tier 2 (MOE2013-T2-2-150 to H.P. Koeffler); the NMRC Centre Grant Programme awarded to National University Cancer Institute of Singapore (NMRC/CG/012/2013 and CGAug16M005) and the National Research Foundation Singapore and the Singapore Ministry of Education under its Research Centres of Excellence initiatives (CSI RCE), and RNA Biology Center at the Cancer Science Institute of Singapore, NUS, as part of funding under the Singapore Ministry of Education's Tier 3 grants (grant number MOE2014-T3-1-006). This research was also supported by the Tower Cancer Research Foundation Michele and Ted Kaplan Family Senior Investigator Grant and Department of Defense USAMRMC (proposal number BM160010, award number W81XWH-17-1-0093), as well as the NCIS Yong Siew Yoon Research Grant through donations from the Yong Loo Lin Trust (to H.P. Koeffler).

The costs of publication of this article were defrayed in part by the payment of page charges. This article must therefore be hereby marked *advertisement* in accordance with 18 U.S.C. Section 1734 solely to indicate this fact.

Received September 5, 2018; revised June 28, 2019; accepted September 16, 2019; published first September 24, 2019.

References

1. Antoni S, Ferlay J, Soerjomataram I, Znaor A, Jemal A, Bray F. Bladder cancer incidence and mortality: a global overview and recent trends. Eur Urol 2017;71:96–108.
2. Allard P, Bernard P, Fradet Y, Tetu B. The early clinical course of primary Ta and T1 bladder cancer: a proposed prognostic index. Br J Urol 1998;81:692–8.
3. Salama A, Abdelmaksoud AM, Shawki A, Abdelbary A, Aboulkassem H. Outcome of muscle-invasive urothelial bladder cancer after radical cystectomy. Clin Genitourin Cancer 2016;14:e43–7.
4. Ploeg M, Kums AC, Aben KK, van Lin EN, Smits G, Vergunst H, et al. Prognostic factors for survival in patients with recurrence of muscle invasive bladder cancer after treatment with curative intent. Clin Genitourin Cancer 2011;9:14–21.
5. Khabar KS. Hallmarks of cancer and AU-rich elements. Wiley Interdiscip Rev RNA 2017;8.
6. Hitti E, Bakheet T, Al-Souhibani N, Moghrabi W, Al-Yahya S, Al-Ghamdi M, et al. Systematic analysis of AU-rich element expression in cancer reveals common functional clusters regulated by key RNA-binding proteins. Cancer Res 2016;76:4068–80.
7. Hudson BP, Martinez-Yamout MA, Dyson HJ, Wright PE. Recognition of the mRNA AU-rich element by the zinc finger domain of TIS11d. Nat Struct Mol Biol 2004;11:257–64.
8. Blackshear PJ, Lai WS, Kennington EA, Brewer G, Wilson GM, Guan X, et al. Characteristics of the interaction of a synthetic human tristetraprolin tandem zinc finger peptide with AU-rich element-containing RNA substrates. J Biol Chem 2003;278:19947–55.
9. Lai WS, Blackshear PJ. Interactions of CCCH zinc finger proteins with mRNA: tristetraprolin-mediated AU-rich element-dependent mRNA degradation can occur in the absence of a poly(A) tail. J Biol Chem 2001;276:23144–54.
10. Lykke-Andersen J, Wagner E. Recruitment and activation of mRNA decay enzymes by two ARE-mediated decay activation domains in the proteins TTP and BRF-1. Genes Dev 2005;19:351–61.
11. Franks TM, Lykke-Andersen J. TTP and BRF proteins nucleate processing body formation to silence mRNAs with AU-rich elements. Genes Dev 2007;21:719–35.
12. Lai WS, Kennington EA, Blackshear PJ. Tristetraprolin and its family members can promote the cell-free deadenylation of AU-rich element-containing mRNAs by poly(A) ribonuclease. Mol Cell Biol 2003;23:3798–812.
13. Schmidlin M, Lu M, Leuenberger SA, Stoecklin G, Mallaun M, Gross B, et al. The ARE-dependent mRNA-destabilizing activity of BRF1 is regulated by protein kinase B. EMBO J 2004;23:4760–9.
14. Adachi S, Homoto M, Tanaka R, Hioki Y, Murakami H, Suga H, et al. ZFP36L1 and ZFP36L2 control LDLR mRNA stability via the ERK-RSK pathway. Nucleic Acids Res 2014;42:10037–49.
15. Maitra S, Chou CF, Luber CA, Lee KY, Mann M, Chen CY. The AU-rich element mRNA decay-promoting activity of BRF1 is regulated by mitogen-activated protein kinase-activated protein kinase 2. RNA 2008;14:950–9.
16. Herranz N, Gallage S, Mellone M, Wuestefeld T, Klotz S, Hanley CJ, et al. mTOR regulates MAPKAPK2 translation to control the senescence-associated secretory phenotype. Nat Cell Biol 2015;17:1205–17.
17. Benjamin D, Schmidlin M, Min L, Gross B, Moroni C. BRF1 protein turnover and mRNA decay activity are regulated by protein kinase B at the same phosphorylation sites. Mol Cell Biol 2006;26:9497–507.
18. Hodson DJ, Janas ML, Galloway A, Bell SE, Andrews S, Li CM, et al. Deletion of the RNA-binding proteins ZFP36L1 and ZFP36L2 leads to perturbed thymic development and T lymphoblastic leukemia. Nat Immunol 2010;11:717–24.
19. Lee SK, Kim SB, Kim JS, Moon CH, Han MS, Lee BJ, et al. Butyrate response factor 1 enhances cisplatin sensitivity in human head and neck squamous cell carcinoma cell lines. Int J Cancer 2005;117:32–40.
20. Planel S, Salomon A, Jalinot P, Feige JJ, Cherradi N. A novel concept in antiangiogenic and antitumoral therapy: multitarget destabilization of short-lived mRNAs by the zinc finger protein ZFP36L1. Oncogene 2010;29:5989–6003.
21. Suk FM, Chang CC, Lin RJ, Lin SY, Liu SC, Jau CF, et al. ZFP36L1 and ZFP36L2 inhibit cell proliferation in a cyclin D-dependent and p53-independent manner. Sci Rep 2018;8:2742.
22. Bell SE, Sanchez MJ, Spasic-Boskovic O, Santalucia T, Gambardella L, Burton GJ, et al. The RNA binding protein Zfp36l1 is required for normal vascularisation

Downloaded from http://aacrjournals.org/cancerres/article-pdf/80/2/219/2796271/219.pdf by guest on 27 August 2022

and post-transcriptionally regulates VEGF expression. Dev Dyn 2006;235: 3144–55.
23. Ciais D, Cherradi N, Bailly S, Grenier E, Berra E, Pouyssegur J, et al. Destabilization of vascular endothelial growth factor mRNA by the zinc-finger protein TIS11b. Oncogene 2004;23:8673–80.
24. Cerami E, Gao J, Dogrusoz U, Gross BE, Sumer SO, Aksoy BA, et al. The cBio cancer genomics portal: an open platform for exploring multidimensional cancer genomics data. Cancer Discov 2012;2:401–4.
25. Edgar R, Domrachev M, Lash AE. Gene Expression Omnibus: NCBI gene expression and hybridization array data repository. Nucleic Acids Res 2002; 30:207–10.
26. Mermel CH, Schumacher SE, Hill B, Meyerson ML, Beroukhim R, Getz G. GISTIC2.0 facilitates sensitive and confident localization of the targets of focal somatic copy-number alteration in human cancers. Genome Biol 2011;12:R41.
27. Silva TC, Coetzee SG, Gull N, Yao L, Hazelett DJ, Noushmehr H, et al. ELMER v.2: An R/Bioconductor package to reconstruct gene regulatory networks from DNA methylation and transcriptome profiles. Bioinformatics 2019;35:1974–7.
28. Davis CA, Hitz BC, Sloan CA, Chan ET, Davidson JM, Gabdank I, et al. The Encyclopedia of DNA elements (ENCODE): data portal update. Nucleic Acids Res 2018;46:D794–D801.
29. Agirre X, Castellano G, Pascual M, Heath S, Kulis M, Segura V, et al. Whole-epigenome analysis in multiple myeloma reveals DNA hypermethylation of B cell-specific enhancers. Genome Res 2015;25:478–87.
30. Qu Y, Siggens L, Cordeddu L, Gaidzik VI, Karlsson K, Bullinger L, et al. Cancer-specific changes in DNA methylation reveal aberrant silencing and activation of enhancers in leukemia. Blood 2017;129:e13–e25.
31. Ronnerblad M, Andersson R, Olofsson T, Douagi I, Karimi M, Lehmann S, et al. Analysis of the DNA methylome and transcriptome in granulopoiesis reveals timed changes and dynamic enhancer methylation. Blood 2014;123:e79–89.
32. Bell RE, Golan T, Sheinboim D, Malcov H, Amar D, Salamon A, et al. Enhancer methylation dynamics contribute to cancer plasticity and patient mortality. Genome Res 2016;26:601–11.
33. Martinez-Calle N, Pascual M, Ordonez R, San Jose-Eneriz E, Kulis M, Miranda E, et al. Epigenomic profiling of myelofibrosis reveals widespread DNA methylation changes in enhancer elements and ZFP36L1 as a potential tumor suppressor gene epigenetically regulated. Haematologica 2019;104:1572–9.
34. Lin DC, Dinh HQ, Xie JJ, Mayakonda A, Silva TC, Jiang YY, et al. Identification of distinct mutational patterns and new driver genes in oesophageal squamous cell carcinomas and adenocarcinomas. Gut 2018;67:1769–79.
35. Vogel KU, Bell LS, Galloway A, Ahlfors H, Turner M. The RNA-binding proteins Zfp36l1 and Zfp36l2 enforce the thymic beta-selection checkpoint by limiting DNA damage response signaling and cell cycle progression. J Immunol 2016;197: 2673–85.
36. Zekavati A, Nasir A, Alcaraz A, Aldrovandi M, Marsh P, Norton JD, et al. Post-transcriptional regulation of BCL2 mRNA by the RNA-binding protein ZFP36L1 in malignant B cells. PLoS One 2014;9:e102625.
37. Rounbehler RJ, Fallahi M, Yang C, Steeves MA, Li W, Doherty JR, et al. Tristetraprolin impairs myc-induced lymphoma and abolishes the malignant state. Cell 2012;150:563–74.
38. Taylor GA, Carballo E, Lee DM, Lai WS, Thompson MJ, Patel DD, et al. A pathogenetic role for TNF alpha in the syndrome of cachexia, arthritis, and autoimmunity resulting from tristetraprolin (TTP) deficiency. Immunity 1996;4: 445–54.
39. Stumpo DJ, Byrd NA, Phillips RS, Ghosh S, Maronpot RR, Castranio T, et al. Chorioallantoic fusion defects and embryonic lethality resulting from disruption of Zfp36L1, a gene encoding a CCCH tandem zinc finger protein of the Tristetraprolin family. Mol Cell Biol 2004;24:6445–55.
40. Stumpo DJ, Broxmeyer HE, Ward T, Cooper S, Hangoc G, Chung YJ, et al. Targeted disruption of Zfp36l2, encoding a CCCH tandem zinc finger RNA-binding protein, results in defective hematopoiesis. Blood 2009;114: 2401–10.
41. Newman R, Ahlfors H, Saveliev A, Galloway A, Hodson DJ, Williams R, et al. Maintenance of the marginal-zone B cell compartment specifically requires the RNA-binding protein ZFP36L1. Nat Immunol 2017;18:683–93.
42. Xu S, Gu G, Ni Q, Li N, Yu K, Li X, et al. The expression of AEG-1 and Cyclin D1 in human bladder urothelial carcinoma and their clinicopathological significance. Int J Clin Exp Med 2015;8:21222–8.
43. Zaharieva BM, Simon R, Diener PA, Ackermann D, Maurer R, Alund G, et al. High-throughput tissue microarray analysis of 11q13 gene amplification (CCND1, FGF3, FGF4, EMS1) in urinary bladder cancer. J Pathol 2003;201: 603–8.
44. Kopparapu PK, Boorjian SA, Robinson BD, Downes M, Gudas LJ, Mongan NP, et al. Expression of cyclin d1 and its association with disease characteristics in bladder cancer. Anticancer Res 2013;33:5235–42.
45. Knowles MA, Hurst CD. Molecular biology of bladder cancer: new insights into pathogenesis and clinical diversity. Nat Rev Cancer 2015;15:25–41.
46. Chen MT, Dong L, Zhang XH, Yin XL, Ning HM, Shen C, et al. ZFP36L1 promotes monocyte/macrophage differentiation by repressing CDK6. Sci Rep 2015;5:16229.
47. Galloway A, Saveliev A, Lukasiak S, Hodson DJ, Bolland D, Balmanno K, et al. RNA-binding proteins ZFP36L1 and ZFP36L2 promote cell quiescence. Science 2016;352:453–9.

Downloaded from http://aacrjournals.org/cancerres/article-pdf/80/2/219/2796271/219.pdf by guest on 27 August 2022